Role of the Linker Domain and the 203–214 N-Terminal Residues in the Human Topoisomerase I DNA Complex Dynamics

G. Chillemi,* M. Redinbo,† A. Bruselles,*‡ and A. Desideri‡

*CASPUR, Consortium for Supercomputing in Research, Via dei Tizii 6b, Rome, Italy; †Department of Chemistry, Department of Biochemistry and Biophysics, University of North Carolina at Chapel Hill, North Carolina; and ‡INFM and Department of Biology, University of Rome ''Tor Vergata'', Via della Ricerca Scientifica, Rome, Italy

ABSTRACT The influence of the N-terminal residues 203–214 and the linker domain on motions in the human topoisomerase I-DNA complex has been investigated by comparing the molecular dynamics simulations of the system with (topo70) or without (topo58/6.3) these regions. Topo58/6.3 is found to fluctuate more than topo70, indicating that the presence of the N-terminal residues and the linker domain dampen the core and C-terminal fluctuations. The simulations also show that residues 203–207 and the linker domain participate in a network of correlated movements with key regions of the enzyme, involved in the human topoisomerase I catalytic cycle, providing a structural-dynamical explanation for the better DNA relaxation activity of topo70 when compared to topo58/6.3. The data have been examined in relation to a wealth of biochemical, site-directed mutagenesis and crystallographic data on human topoisomerase I. The simulations finally show the occurrence of a network of direct and water mediated hydrogen bonds in the proximity of the active site, and the presence of a water molecule in the appropriate position to accept a proton from the catalytic Tyr-723 residue, suggesting that water molecules have an important role in the stabilization and function of this enzyme.

INTRODUCTION

Topoisomerases are a ubiquitous family of enzymes essential for the control of DNA supercoiling generated by replication, transcription, and recombination. Eukaryotic topoisomerase I enzymes relax DNA superhelical tension by introducing a transient single-strand break in one strand of duplex DNA and forming a covalent phosphotyrosyl bond with the 3′-end of the broken DNA strand. The covalent topoisomerase-DNA complex is the molecular target of the anti-tumor drug camptothecin (CPT) (Pommier et al., 1999) that stabilizing it produces DNA damage after collisions with replication forks or transcription complexes (Pommier et al., 2003). Human topoisomerase I is composed by four domains: the N-terminal, the core (formed by three subdomains), the linker, and the C-terminal domain, which includes the catalytic tyrosine 723. Several crystal structures of N-terminal truncated forms of the protein have revealed that the enzyme wraps completely around duplex DNA to induce a single-strand break. The topoisomerase I catalytic cycle is composed of five subsequent steps: DNA binding; DNA cleavage; relaxation of superhelical tension; DNA religation; and DNA release (Pommier et al., 1998). During these steps the enzyme goes through large conformational variations without any need for energy cofactors, from an ''open'' structure that allows the DNA binding, to the ''close'' conformations observed by x-ray diffraction in which the enzyme completely embraces the DNA. The importance of topoisomerase I flexibility in the modulation of the enzymatic catalysis has been elegantly pointed out by two recent works describing the properties of the enzyme cross-linked through a disulfide bridge either at the salt-bridge loops (Carey et al., 2003) or at the active-site proximal loops (Woo et al., 2003).

The large conformational dynamics implied by the catalytic cycle of the enzyme can in principle be described through MD simulations designed to investigate the structural and dynamical properties of proteins and nucleic acids (Tsui et al., 2000; MacKerell and Nilsson, 2001; Giudice and Lavery, 2002). Recently, we have used this approach to investigate a covalent human topoisomerase I-DNA complex involving a form of the enzyme lacking the N-terminal domain (resides 1–214) and linker domain (residues 627–719; topo58/6.3). These studies provided information on the protein-DNA interactions and the role of water in protein-DNA recognition and in catalysis (Chillemi et al., 2001), and permitted us to demonstrate the occurrence of intra- and interdomain communications between topo58/6.3 regions (Chillemi et al., 2003).

Recent structural and functional data have highlighted the importance of the N-terminal residues 203–214 and the linker domain on topoisomerase I activity and CPT sensitivity (Stewart et al., 1999; Ireton et al., 2000; Redinbo et al., 2000; Lisby et al., 2001; Frohlich et al., 2004). Moreover, certain conformations of the enzyme appear able to perturb the dynamical properties of the linker domain. For example, this domain is disordered in many binary topoisomerase I-DNA complexes (e.g., Redinbo et al., 1999; Staker et al., 2002), but it is visible in the ternary complex of human topoisomerase I, DNA ,and the camptothecin analog topotecan (Staker et al., 2002). In accordance with this, we have recently shown that a mutation within the linker domain that

Submitted April 26, 2004, and accepted for publication August 25, 2004.

Address reprint requests to A. Desideri, Dept. of Biology, University of Rome Tor Vergata, Via della Ricerca Scientifica, 00133 Rome, Italy. Tel.: 39-06-72594376; Fax: 39-06-72594326; E-mail: desideri@uniroma2.it.

0006-3495/04/12/4087/11 $2.00

doi: 10.1529/biophysj.104.044925

confers CPT resistance increases greatly the mobility of this domain (Fiorani et al., 2003). Thus, it is clear from several lines of evidence that the linker domain and regions of the N-terminal domain play important roles in the catalytic action of topoisomerase I.

We have now investigated the impact of the N-terminal residues 203–214 and the linker domain on the dynamics of human topoisomerase I by comparing the topo70-DNA covalent complex (containing these regions) with the topo58/6.3-DNA covalent complex (Fig. 1). Simulations of the topo70 system revealed a complex network of correlated and anticorrelated motions not observed in the topo58/6.3-DNA system. These observations suggest that only the form of the enzyme containing amino acids 203–765 can accurately control all steps of catalysis, particularly the DNA strand cleavage and the proposed controlled rotation relaxation of DNA supercoils.

METHODS

The starting coordinates of the topo58/6.3-DNA covalent complex were obtained from the crystal structure 1a31 (Redinbo et al., 1998). The topo70-DNA covalent complex was modeled obtaining the starting position for residues 215–633 and 641–765 from the crystal structure 1a36 (Stewart et al., 1998), and those for residues 203–214 from the crystal structure 1ej9 (Redinbo et al., 2000). The five residues constituting the loop region that connects the linker to the core domain (residues 636–640), which are lacking in the 1a36 Protein Data Bank (PDB) structure because of thermal fluctuation, and the covalent bond between Tyr-723 and the DNA-1 base were added to the system by molecular modeling. The spatial environment of each new residue was checked for close contact or overlap with neighboring residues and stereochemical regularization of the structures was obtained by the Powell minimization method implemented in the SYBYL program (Tripos, St. Louis, MO). At the moment this procedure was adopted, it was the only way to obtain a structure of human topoisomerase I residues 203–765 in covalent complex with DNA. Successively, the x-ray structure of the ternary complex topo70-DNA–Topotecan has been solved (1K4T; Staker et al., 2002). However, the backbone root mean-square deviations of our model, respective to the 1K4T x-ray structure, is only 1.6 Å.

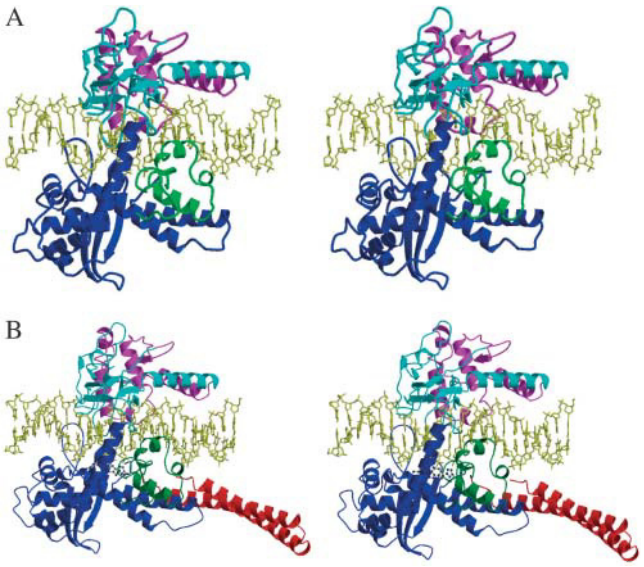

FIGURE 1 (*A*) Topo58/6.3 human topoisomerase I structure in complex with duplex DNA. Core Subdomains I, II, and III are rendered in cyan, magenta, and blue, respectively, whereas the C-terminal domain is in green and the DNA duplex in yellow. (*B*) Topo70 human topoisomerase I structure in complex with duplex DNA. Colors are as in panel *A*, with the addition of the linker domain in red. The active site residues are shown in light and dark gray.

The systems were modeled with the AMBER95 all-atom force field (Cornell et al., 1995) and immersed in a rectangular box ($105 \times 92 \times 99$ and $127 \times 84 \times 108$ Å^3 for topo58/6.3 and topo70, respectively) filled with TIP3P water molecules (Jorgensen et al., 1983). The protein residue ionization state has been assigned considering the most probable one at neutral pH, i.e., lysine and arginine residues are protonated; aspartate and glutamate residues are deprotonated; histidine residues are half protonated. Na^+ counterions have been added to make the system electro-neutral. The resulting total systems contained 7,679 protein atoms, 1,401 DNA atoms, 27 Na^+ counterions, and 23,216 water molecules for topo58/6.3, giving a total of 78,755 atoms; 9417 protein atoms, 1,401 DNA atoms, 21 Na^+ counterions, and 28,313 water molecules for topo70, giving a total of 95,778 atoms. It is worth noting that these great dimensions ask for efficient parallel computers to be simulated. Simulation of the topo70-DNA complex for 3250 ps has required, for example, 408 h of wall clock time on 8 CPUs of the IBM sp4 (Power4 @ 1.3 GHz). The systems were simulated in periodic boundary conditions, using a cutoff radius of 9 Å for the nonbonded interactions, and updating the neighbor pair list every 10 steps. The electrostatic interactions were calculated with the particle mesh Ewald method (Darden et al., 1993; Cheatham et al., 1995). The SHAKE algorithm (Ryckaert et al., 1977) was used to constrain all bond lengths involving hydrogen atoms. Optimization and relaxation of solvent and ions were initially performed keeping the solute atoms constrained to their initial position with decreasing force constants of 500, 25, 15, and 5 Kcal/(mol Å). The systems have been simulated for 3250 ps at a constant temperature of 300 K using Berendsen's method (Berendsen et al., 1984) and at a constant pressure of one bar with a 2 fs time step. Pressure and temperature coupling constants were 0.5 ps. The analyses reported in this manuscript refer to the last 3000 ps of the trajectory (i.e., from 250 to 3250 ps), since the trend of the root mean-square deviations indicates that the systems were well stabilized after 250 ps.

The dynamic cross-correlation (DCC) maps of the systems were built with in-house written code, taking into account the coordinates of the protein C-α atoms since they contain enough information to describe the largest system motions. The elements of the dynamic cross-correlation map (C_{ij}) were computed as:

$$C_{ij} = \frac{\langle \Delta r_i \times \Delta r_j \rangle}{\sqrt{\langle \Delta r_i^2 \rangle} \times \sqrt{\langle \Delta r_j^2 \rangle}},$$

where Δr_i is the displacement from the mean position of the ith atom and the $\langle\ \rangle$ represent the time average over the whole trajectory (Mc Cammon and Harvey, 1987). Positive C_{ij} values represent a correlated motion between residues *i* and *j* (i.e., the residues move in the same direction). Negative values of C_{ij} represent an anticorrelated motion between residues *i* and *j* (i.e., they move in opposite directions). The order parameter and the direct hydrogen bonds have been calculated using the GROMACS MD package version 3.1.4 (Berendsen et al., 1995). The water-mediated hydrogen bond calculation was made using an in-house written code, based on the GROMACS code.

RESULTS AND DISCUSSION

Backbone fluctuations

The per residue backbone fluctuations for the topo70 and topo58/6.3 systems are shown in Fig. 2. Topo58/6.3

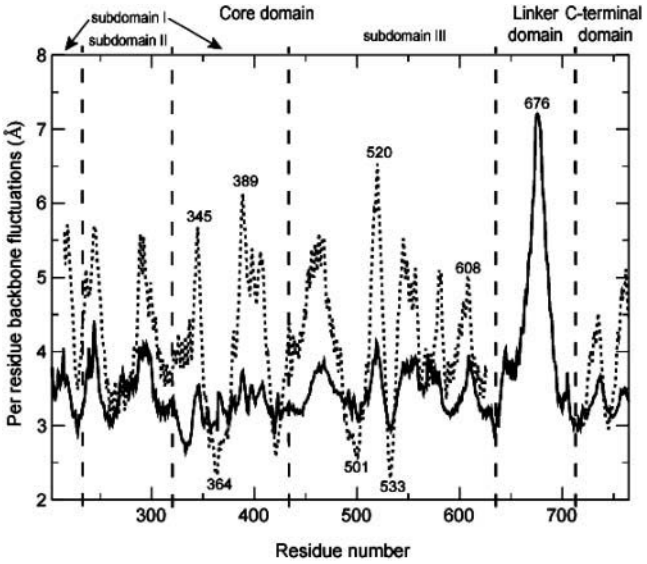

FIGURE 2 Per residue root mean-square fluctuations for topo70 (*full line*) and topo58/6.3 (*dotted line*). Residues with high or low fluctuations are indicated.

fluctuates more than topo70 (average fluctuation of 4.1 Å vs. 3.5 Å) even though the linker domain in topo70 contains the residues with the largest range of fluctuation, reaching values higher than 7 Å in the loop connecting helices 18 and 19 (Fig. 1 *B*). Such observations indicate that the presence of the linker domain and of the N-terminal residues dampen the fluctuations of the core and C-terminal domains. A similar trend is observed in the crystallographic thermal displacement parameters (*B*-factors), an experimental measure of protein mobility. The linker domain in the 1a36 crystallographic structure is the most mobile region (average *B*-factor of 60.5 $Å^2$) and its presence reduces the relative *B*-factors of the core and C-terminal domains. The mean *B*-factors of the core and C-terminal domain are 37.3 and 42.6 $Å^2$, respectively, in the presence of the linker domain, whereas in the absence of the linker domain (crystallographic structure 1a31) the mean *B*-factors are 48.3 and 55.0 $Å^2$, respectively. The mean *B*-factors over all atoms for the topo70-DNA (1a36) and topo58/6.3-DNA (1a31) complex structures are 48.9 and 40.9 $Å^2$, respectively.

The presence of the linker domain also dampens individual fluctuations within the human topoisomerase I DNA complex. For example, fluctuations in topo58/6.3 are characterized by more extreme minima and maxima values than in topo70 (Fig. 2). This phenomenon is more evident in core subdomain I, where topo70 has average and standard deviation fluctuations of 3.2 and 0.2 Å, whereas the respective topo58/6.3 values are 4.0 and 0.9 Å (Fig. 2). In both systems, Asn-345 and Asp-389 are the most fluctuating residues in this protein region, but their fluctuations are greatly reduced in topo70. The most dramatic dynamical changes occur in the region located between these two residues. Arg364, in fact, has very low fluctuations in topo58/6.3 but not in topo70. Analyses presented below confirm these data, indicating that the linker domain and the N-terminal residues strongly perturb the dynamics of the Phe-361–Lys-369 region that constitutes lip1, one of the two lips on the core of the enzyme that clamp around DNA. The fluctuations of core subdomain II are also strongly dampened (Fig. 2). The average fluctuations and standard deviation of this subdomain are 3.0 and 0.3 Å, respectively, in topo70 compared with 3.6 and 0.8 Å, respectively, in topo58/6.3.

The decrease of the average fluctuations and standard deviation is nearly the same in core subdomain III (average and standard deviation fluctuations of 3.5 and 0.3 Å, respectively, in topo70, versus 4.2 and 0.8 Å in topo58/6.3) (Fig. 2). In this protein region, some key residues maintain the same relative behavior in both simulations (e.g., 519–520 and 608–609, which show high fluctuations, and Asp-533, which exhibits low fluctuations). Asp-533 is the only protein residue found crystallographically to contact directly the camptothecin derivative Topotecan (Staker et al., 2002).

The C-terminal domain fluctuates less in topo70 than in topo58/6.3 (average and standard deviation fluctuations of 3.3 and 0.2 Å, respectively, in topo70, versus 3.9 and 0.6 Å in topo58/6.3) and the relative maxima and minima fluctuations are almost completely maintained (Fig. 2). The DNA fluctuations do not show significant difference in the two simulations, with average fluctuations and standard deviation of 3.4 and 0.9, respectively, in topo58/6.3, versus 3.5 and 0.7 Å in topo70. This agrees with the mean crystallographic *B*-factors of DNA atoms, which are 47.1 and 48.3 $Å^2$, respectively, for 1a31 and 1a36 crystallographic structures.

S^2 parameter for Φ/Ψ dihedral angles

The flexibility of the protein backbone has also been examined through the calculation of an order parameter S^2, which is related to the protein Φ/Ψ backbone dihedral angles (Van der Spoel and Berendsen, 1997). S^2 gives a measure of the flexibility of the backbone, being 1 in a completely rigid system, or 0 in a system where all the possible conformations are sampled. The order parameter for topo70 and topo58/6.3, shown in Fig. 3, indicates that the backbone of both structures is quite rigid, with relatively few residues exhibiting S^2 values <0.7.

In topo70, Glu-213 and Gly-214, two residues not present in the topo58/6.3 simulation, display a very high flexibility, with the S^2 values for their respective Ψ and Φ dihedral angles being 0.26 and 0.28. These residues are located at the C-terminal of the 12 N-terminal residues that were first detected through x-ray diffraction in the topo58/6.3-DNA complex where a cytosine rather than the favored thymine is present at the −1 position of the scissile strand (PDB id 1ej9; Redinbo et al., 2000). These residues have since been observed in other structures of topo70 in complex with DNA

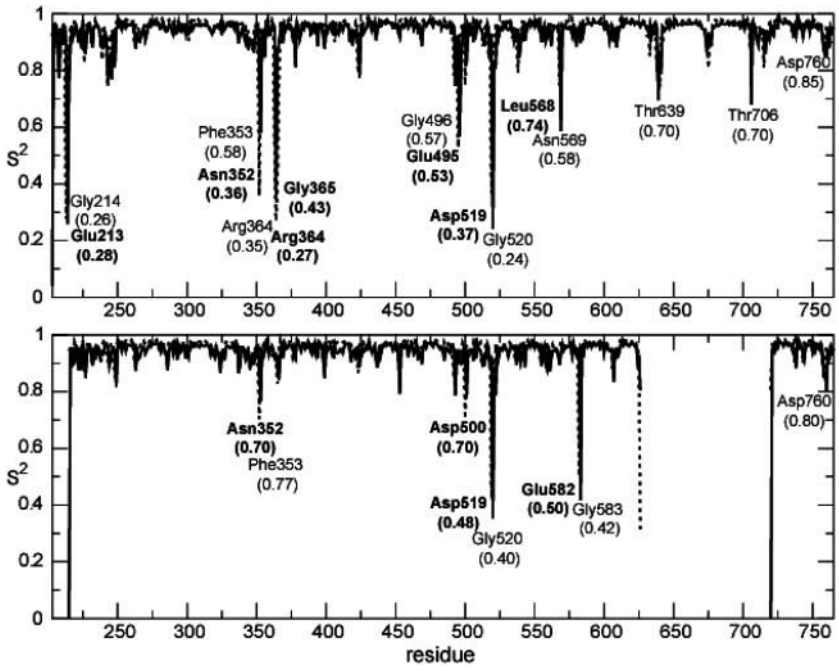

FIGURE 3 ϕ/ψ Order Parameter S^2 for topo70 (*upper panel*) and topo58/6.3 (*lower panel*). ϕ and ψ dihedral angles are represented in full and dotted lines, respectively. Residues with low S^2 value are indicated, with their respective ϕ/ψ S^2 value in brackets (bold characters are used for ψ dihedral angles).

(e.g., 1K4T, 1K4S, Staker et al., 2002; 1NH3, Chrencik et al., 2003; 1LPQ, Lesher et al., 2002). Inspection of the Ramachandran plots shows that Glu-213/Gly-214 visit two different backbone conformations sampled for 1000 ps and 2000 ps of simulation time (data not shown).

The Asn-352/Phe-353 region is flexible in both topo70 and topo58/6.3. In the topo70 simulation, the S^2 value for the respective Ψ/Φ dihedral angles are slightly lower than the corresponding values in topo58/6.3 (0.36/0.58 in topo70 vs. 0.70/0.77 in topo58/6.3), indicating that in both systems a great number of Ψ angle values are sampled by Asn-352 during the simulation. The high flexibility of the Asn-352 backbone may be related to the antitumor activity of SN-38 (a camptothecine analog) relative to the parent compound. Upon mutation of Asn-352 to alanine, SN-38 shows a decreased ability to poison the human topoisomerase I-DNA complex, whereas CPT's efficacy is unchanged. It has been suggested that the loss of a direct hydrogen bond between Ala-352 and the A-ring 10-OH atom, present in SN-38 but not in CPT, may explain this observation (Laco et al., 2002). Asn-352 is located adjacent to the A ring 9-group CH2-N$(CH_2)_2$, in the recently solved ternary topo70-DNA-Topotecan 3D structure (Staker et al., 2002) and not hydrogen-bonded to the 10-OH atom, which is also present in Topotecan. Despite the absence of this bond, the proximity of Asn-352 to the 9- and 10-position on the camptothecins suggests that the backbone flexibility of this residue observed in our simulations could play an important role in topoisomerase-camptothecin drug interactions. It is interesting to note that, despite the flexibility of its main chain, the side chain of Asn-352 forms two stable hydrogen bonds with Tyr-426 and Met-428 in both simulations.

The backbone dynamics of Arg-364 and Gly-365 show a high flexibility in topo70 (Arg-364 S^2 values of 0.35 and 0.27 for Φ and Ψ, respectively; Gly-365 S^2 values of 0.43 for Ψ) but not in topo58/6.3 (Arg-364 S^2 values of 0.93 and 0.92 for Φ and Ψ, respectively; Gly-365 S^2 values of 0.83 for Ψ), demonstrating an influence of the linker domain in the motion of these residues. As already pointed out, Arg-364 is less fluctuating in topo58/6.3 than in topo70 (2.4 vs. 3 Å; see Fig. 2). The order parameter analysis shows that the increased fluctuation in topo70 is coupled to a dramatic increase in the backbone flexibility of this residue. The position of Arg-364 appears to be critical to the productive binding of the camptothecins to human topoisomerase I (Staker et al., 2002; Chrencik et al., 2004).

High flexibility is also found in the Asn-491/Thr-501 lip2 region of core subdomain III in topo70 but not in topo58/6.3. Several lip2 residues in topo70, in fact, show S^2 values lower than 0.8, (minimum of 0.53/0.57 for the Glu-495/Gly-496 Ψ/Φ dihedral angles), whereas only Asp-500 shows an S^2 value equal to 0.7 in topo58/6.3. The average fluctuations of lip2 residues are also increased in topo70 compared to topo58/6.3 (see Fig. 2). Therefore, the two lips show a similar behavior: low fluctuations and rigid backbone in topo58/6.3; large fluctuations, although always less than the average; and flexible backbone in topo70.

The Asp-519/Gly-520 couple is very flexible in both systems, with Ψ/Φ S^2 values lower than 0.5 (see Fig. 3). These residues, located in the loop between β12 and β13, display relative maximum fluctuations followed by a relative minimum at the Asp-533 residue (see Fig. 2). It is interesting to notice that these well-conserved dynamical features involve a region containing essential residues, such as Asp-533,

whose mutation in Gly or Asn produces CPT resistance (Andoh et al., 1987; Tamura et al., 1991; Saleem et al., 1997), or Lys-532, the only amino acid forming a base-specific contact with DNA (Redinbo et al., 1998, 2000). Asp-533 is the only amino acid side chain that directly contacts the camptothecin analog topotecan, as observed in a crystal structure of the topoisomerase I-DNA-topotecan complex (Staker et al., 2002). The principal component analysis, a technique used to identify large collective protein movements connected to functional properties, showed that the flexibility in the Asp-519/Gly-520 backbone of topo58/6.3 is functionally connected to the motion of the β12-β13-β14 sheet (Chillemi et al., 2003, and supplementary material therein). This movement permits the direct insertion and removal of helix 13, containing Lys-532 and Asp-533, in the DNA minor groove and its participation in the active site orientation (Chillemi et al., 2003).

The backbone of Leu-568/Asn-569 is also significantly flexible in topo70, being 0.74/0.58 the S^2 values for their respective Ψ/Φ dihedral angles, but not in topo58/6.3. These residues connect the 550–567 region, which exhibits motion strongly correlated with the linker domain (see below), to helix 15 (residues 570–580). The backbone flexibility of Leu-568/Asn-569 permits the uncoupling of the motion between helix 15 and the 550–567 region in topo70. In contrast, such flexibility is not observed in topo58/6.3, since the deletion of the linker domain abolishes the stimulus on the 550–567 region. On the other hand, Glu-582/Gly-583 have low S^2 values in topo58/6/3 (0.50/0.42 for the respective Ψ/Φ dihedral angles), and rigid backbone in topo70 (0.92/0.90 S^2 values for the respective Ψ/Φ dihedral angles). The backbone flexibility of Glu-582/Gly-583 permits the mechanical uncoupling of helices 16 and 15.

The linker domain, the most fluctuating region in topo70, does not have a flexible backbone because its two long helices appear to move as a whole and to not contain a hinge residue. The residues with lower S^2 value are Thr-706 and Thr-639. The latter one is located in the loop connecting the core with the linker domain that is disordered in the 1a36 PDB structure. The C-terminal domain is quite rigid in its backbone motion and the S^2 values are very similar in the two simulations, with a lower S^2 value located on Asp-760.

DCC map

The dynamic cross correlation (DCC) map for the two simulations is shown in Fig. 4. The map values (C_{ij}) are a measure of the correlated motion between residues i and j. Positive C_{ij} values are indicative of strong correlation in the movement of residues i and j in the same direction, whereas negative C_{ij} values denote that the two residues move along opposite direction (anticorrelated motion). The analysis has been carried out on the protein Cα atoms since they contain enough information to describe the largest protein motions. The intensity of the correlation has been color coded, as described in Fig. 4, where the 563 C_{ij} values for topo70 (residues 203–765) are reported in the upper left triangle of Fig. 4, and the corresponding 458 C_{ij} values for topo58/6.3 (residues 215–626 and 720–765) in the lower right triangle. The dimensions of the systems ($\sim$100,000 atoms) and the intrinsic flexibility of the topoisomerase enzyme exclude the possibility to visit, during the simulation, the whole conformational space available to the protein. Nevertheless, the DCC map analyses provided useful information, highlighting the role of specific residues in the protein-protein and protein-DNA communications (Chillemi et al., 2003; Reddy et al., 2003). In the following, we will limit our description to the DCC map peaks having an absolute value >0.5, that are observed after 2 ns (data not shown) and remain greater than the cutoff after 2.5 (data not shown) and 3 ns (Fig. 4), under the hypothesis that they represent the main motion fingerprint of the system. These peaks are also identified in a comparative analysis concerning the first (0.25–1.75 ns) and second (1.75–3.75 ns) halves of the trajectory. Therefore we will not discuss correlation peaks observed after 3 ns that were not already higher than the cutoff in the previous times.

The three-dimensional structure of the 12 amino terminal residues show that they lie close to helix 8 (residues 434–453), which has been hypothesized to be a hinge in the clamping of the enzyme around DNA (Redinbo et al., 2000). It is not surprising, then, to observe a strong correlation in the motion of residues 203–207 with residues 430–448 in helix 8 (see *ellipse A* in Fig. 4). The same N-terminal residues show direct correlated motions with the catalytic region of Tyr-723 and residues 743–755 in helices 23 and 24 of the C-terminal domain, highlighted in ellipse *C*. These last two correlated motions cannot be explained by direct contacts and they imply a long-range communication. In fact, the sole stable protein-protein hydrogen bond between residues 203–214 and the rest of the protein is formed by Trp-206 and Asp-757, for 82% of the simulated time. Moreover, residues 203–207 show significant anticorrelated motions with residues 677–693, i.e., with the N-terminal portion of helix 19 in the linker domain (*ellipse B*).

Residues of the linker domain show different dynamics depending on their position. The N-terminal portion of the domain (residues 636–648) has correlated motion with its C-terminal portion (residues 698–712), highlighted in square *D*. Both these regions have correlated motion with the C-terminal portion of the core subdomain III, as highlighted by rectangles *E* and *F*. The motion highlighted in rectangle *E* involves a region of core subdomain III (residues 595–627) smaller than rectangle *F* (residues 597–634), indicating that only the N-terminal portion of the linker domain exerts a direct influence on the catalytic His-632 dynamics.

The central portion of the linker domain (residues 657–691) behave like a rigid body, with high correlated motions among its residues (DCC map values always >0.7 and frequently >0.85, respectively, in *yellow* and *red* color in Fig. 4). This portion of the linker domain shows anticorrelated

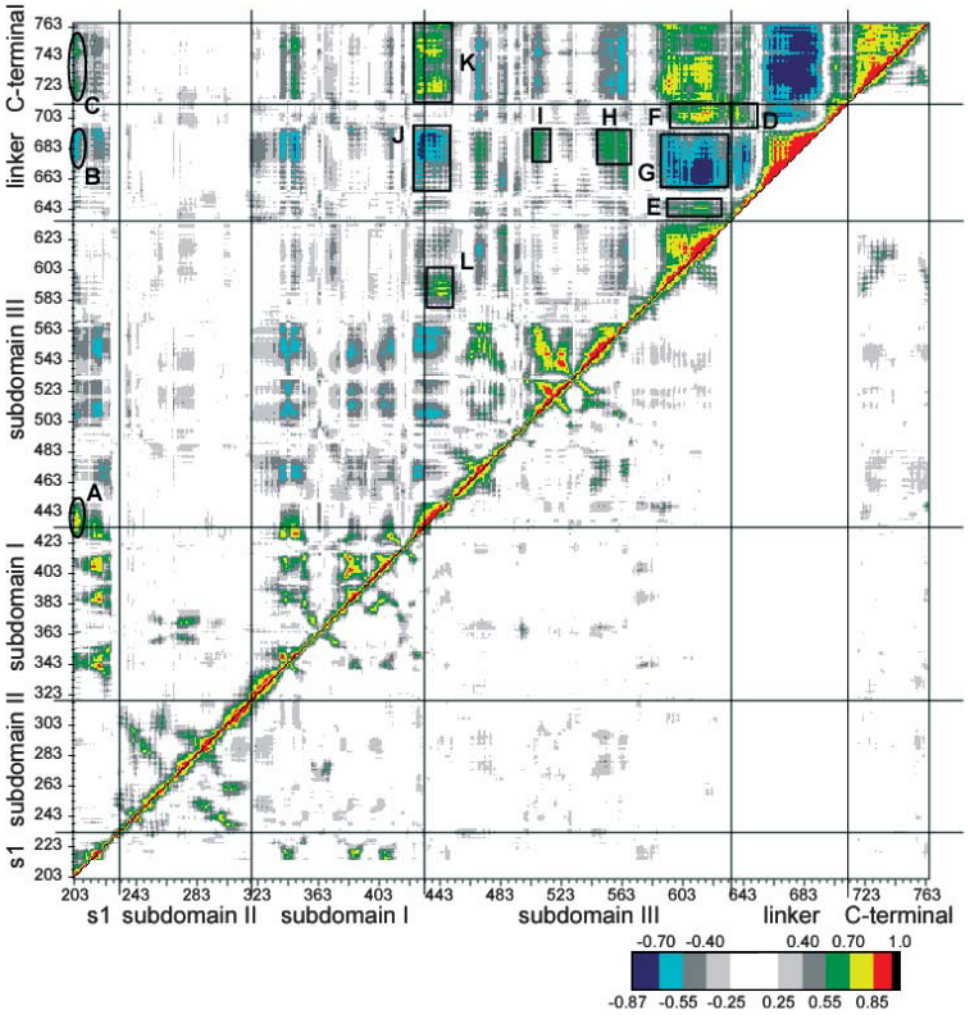

FIGURE 4 Dynamic cross correlation map for the topo70 (*upper left triangle*) and topo58/6.3 (*lower right triangle*). Correlated values with $0.55 \leq C_{ij} < 0.70$, $0.70 \leq C_{ij} < 0.85$ and $0.85 \leq C_{ij} < 1$ are represented in green, yellow, and red, respectively, whereas the anticorrelation values $-0.70 \leq C_{ij} < -0.55$ and $-0.8 \leq C_{ij} < -0.70$ are represented in cyan and blue, respectively. The correlation range $0 \leq C_{ij} < 0.55$ and the anticorrelation range $-0.55 \leq C_{ij} < 0$ are represented in a gray scale depending on the absolute value of the correlation. The value 1, along the diagonal (correlation of the residue with itself), is represented in black.

motions with the N-terminal portion of the linker itself, the whole C-terminal domain, the C-terminal portion of the core subdomains III (*square G*) and residues 429–448, in helix 8 of core subdomain III (highlighted in *rectangle J*), proposed as the region involved in the opening and closure of the enzyme around the DNA (Redinbo et al., 1998). The same portion of the linker domain shows correlated motions with the C-terminal and N-terminal portions of the region containing the β12-β13-β14 sheet and helix 13 (highlighted by *rectangles H* and *I*, respectively).

Helix 8, besides the anticorrelated motion with the linker domain and the correlated one with the N-terminal residues 203–207, shows correlated motion with nearly the whole C-terminal domain (highlighted in *rectangle K*) and with residues 581–602 in helix 16 of the core subdomain III (highlighted in *rectangle L*), containing the catalytic residue Arg-590.

Inspection of topo70 DCC map reveals a network of strong correlated and anticorrelated motions among key residues. These correlated motions involve most of the protein regions indicated as playing a role in the enzymatic cycle (Redinbo et al., 1998; Stewart et al., 1998; Frohlich et al., 2004): the C-terminal domain, in particular the Tyr-723 catalytic region; the linker domain; helix 8 in core subdomain III; the 203–207 N-terminal residues. In topo58/6.3 correlated motions between helix 8 in core subdomain III and the whole C-terminal domain or helix 16 are completely absent, whereas the whole topo70 form of the enzyme show very high peaks (highlighted in *rectangles K* and *L*, respectively), providing a structurally dynamical interpretation for its highest DNA relaxation activity (Stewart et al., 1997; Lisby et al., 2001). Indeed, topo58/6.3 and all the enzyme forms in which the linker domain has been disabled show an increase in the religation rate, and a distributive behavior, i.e., they produce many partially relaxed topoisomers, reflecting a reduced affinity for DNA (Ireton et al., 2000; Fiorani et al., 2003).

Hydrogen bonding at the active site

Analysis of the simulations in proximity of the active site indicates the occurrence of a stable network of hydrogen

bonds, both direct and water mediated, that likely plays an important role in the communication between protein and DNA. The presence of long residence water molecules is particularly interesting since a catalytic mechanism has been proposed where the solvent molecule would serve as a specific base to activate the catalytic Tyr-723 residue (Stewart et al., 1998; Redinbo et al., 2000; Bailly, 2003). Molecular dynamics simulation of the topo58/6.3-DNA complex supports this hypothesis since four out of 17 long residence water molecules are localized in the proximity of the active site, indicating that this region behaves as a water attractor (Chillemi et al., 2001). Moreover, one of these water molecules is hydrogen bonded to the phosphate group involved in the covalent attachment of Tyr-723 to the −1 DNA scissile base (PTR723), and therefore in the appropriate position to participate to the catalytic reaction (Chillemi et al., 2001).

Significantly, a water molecule is present also in the topo70 active site (shown in Fig. 5), for nearly all the simulation time, again in an appropriate position to accept a proton from Tyr-723. This water molecule forms the following water mediated bonds: PTR723-His-632, PTR723-Arg-488 and Arg-488–His-632 for 91%, 84%, and 79% of simulation time, respectively. Moreover, both Arg-590 and Lys-532 are hydrogen bonded with a single water molecule for 89 and 93% of simulation time, respectively, thus contributing to maintaining long-residence water molecules in the active site region. These results indicate a synergistic role for Tyr-723, Arg-488, Arg-590, Lys-532, and His-632 residues in the formation and stabilization, together with water molecules, of the pentacovalently coordinated transition state, as already suggested by crystallographic data and biochemical experiments (Bailly, 2003).

Fig. 5 shows a snapshot of the topo70 active site representative of the simulation, in which the majority of the stable hydrogen bonds involving protein residues and DNA bases around the topoisomerase active site are highlighted. In detail, the phosphate group covalently bonded to PTR723 forms with its O1P oxygen two direct hydrogen bonds with the +1 A 5′-OH, and with Arg590 for the 94% and 96% of the simulation time, respectively. The +1 A 5′-OH also forms a water-mediated hydrogen bond with the phosphate PTR group, although only for 11% of the simulation time. These two bonds could be significant in the religation phase of catalysis when the 5′ oxygen must reform the covalent bond with the phosphate group.

Lys-532 plays an important role in the catalytic reaction, recently better clarified by means of mutagenesis experiments (Interthal et al., 2004). This residue contacts the O2 atom of the scissile base in the crystallographic structures of both topo58/6.3 (PDB id 1a31 and 1a35) and topo70 (PDB id 1a36, 1ej9, 1nh3, 1k4s, 1k4t, 1lpq) but mutation of Lys-532 in arginine or alanine has demonstrated that this interaction is not required for DNA sequence specificity (Interthal et al., 2004). The same study indicates that Lys-532 behaves as a general acid, in the cleavage reaction, protonating the leaving 5′ oxygen. Both the topo58/6.3 and topo70 simulations confirm the direct stable hydrogen bond between Lys-532 and the O2 atom of the −1 scissile base, but the topo70-DNA complex simulation shows three other Lys532-DNA contacts: with the O4′ atom of the +1 A base in the scissile strand, for 51% of the simulation time; with the N3 atom of the A −1 base in the intact strand, for 10% of the simulation time; and with the N3 atom of the A −2 base in the intact strand, for 81% of the simulation time. Interestingly, all the topo70 crystallographic structures show that Lys-532 is able to contact several DNA bases, either in the scissile (−1 and +1 bases) or in the intact strand (−2 and −3 bases).

In several crystallographic structures of topo70 (PDB id 1a36, 14ks, 1k4t) the side chain of Thr-718 is hydrogen bonded with the phosphate group of G +2 of the scissile strand. Staker and coauthors suggest that this interaction may help the positioning of the +1 5′-OH to allow the nucleophilic attack of PTR723 in the religation step (Staker et al., 2002), thus explaining the lethal phenotype of a Thr-718 to Ala mutation that kills the cell upon stabilizing the topoisomerase-DNA covalent intermediate, similarly to CPT (Fiorani et al., 1999). The topo70-DNA complex simulation not only confirm the high stability of the hydrogen bond between Thr-718 and the G +2 phosphate group, present for the whole simulation, but it also shows that the catalytic residues Arg-488 and His-632 form additional highly stable hydrogen bonds with the same phosphate group (Fig. 5), indicating that the enzyme accurately controls the relative position of the +1 base with regard to the active site, by means of several direct hydrogen bonds with the +2 G phosphate group.

The importance of Asn-722 has been demonstrated by several experimental studies. Mutation of this residue to leucine results in a decrease of enzymatic activity, whereas its mutation to Ala leads to resistance to CPT and other topoisomerase poisons (Knab et al., 1993; Knab et al., 1995; Hann et al., 1998). Mutations to Ser, Asp, or His interfere with both enzyme activity and drug sensitivity (Leteurtre et al., 1994; Fertala et al., 2000). Crystal structures of topoisomerase-DNA covalent complexes indicate that this residue, depending on the experimental conditions, is able to form hydrogen bonds with the phosphate oxygen atoms of −1 T (PDB id 1k4s), with the O5′ oxygen of +1 G (PDB id 1nh3) or with the O4′ and O5′ oxygen atoms of +1 T (PDB id 1a31). Moreover, the topoisomerase-DNA-Topotecan ternary structure shows a water mediated contact between Asn-722 and the Topotecan drug (Staker et al. 2002). Our simulation shows that Asn-722 can influence the position of the two scissile DNA bases (−1 and +1), through a direct hydrogen bond with the OP oxygen atoms of −1 T for the whole simulation and a water-mediated bond with the N7 atom of +1 A for 80% of the simulation time. These

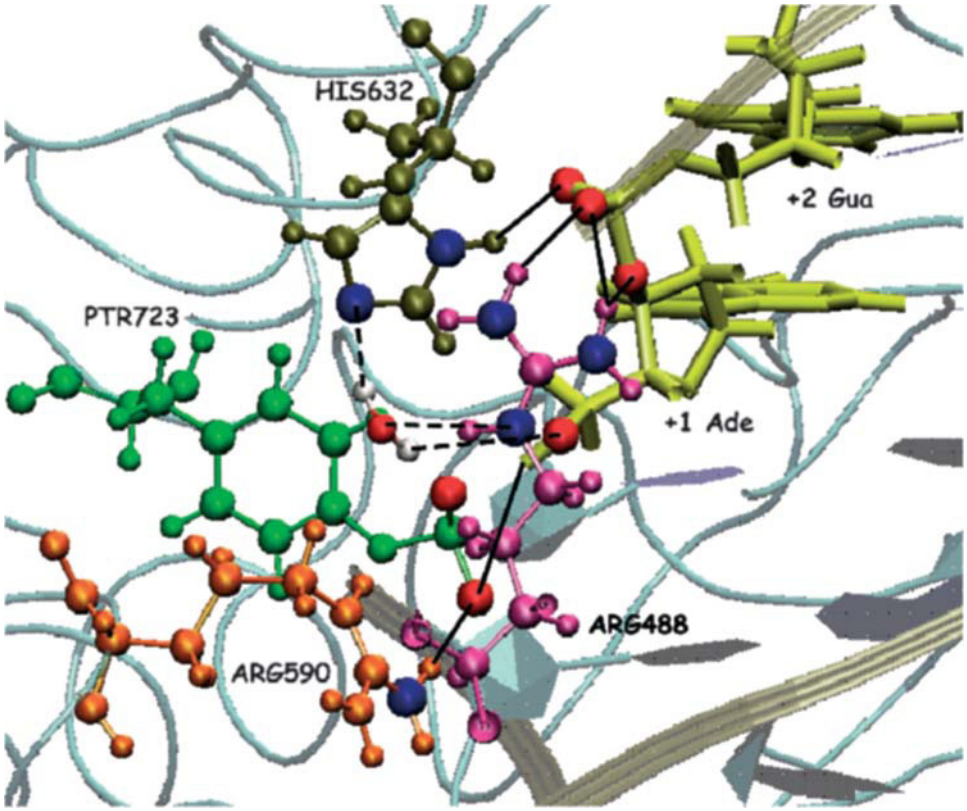

FIGURE 5 Molecular dynamics snapshot of the active site region. The active site residues and bases are highlighted in different color; the oxygen and nitrogen atoms involved in the hydrogen bonds are represented in red and blue, respectively. Direct and water-mediated hydrogen bonds are represented in black full and dashed lines, respectively.

observations support the importance of this residue for topoisomerase activity and drug sensitivity.

CONCLUSIONS

The simulations reported here highlight the crucial role played by the linker domain and the N-terminal residues in human topoisomerase I, allowing us to shed some light on the complex structural dynamics involved in the action of this enzyme. The topo70-DNA complex simulation shows the occurrence of specific correlated motions that differ significantly from the ones previously found in the topo58/6.3 simulation (Chillemi et al., 2003). These results demonstrate that the presence of these regions deeply alters the dynamics of specific key protein regions. A dynamical coupling between the linker domain and the active site can be envisaged from the x-ray structure of topo70 system in the presence and absence of Topotecan since the linker domain cannot be visualized in the binary topoisomerase-DNA complex but it is visible in the ternary topoisomerase-DNA-Topotecan complex (Staker et al., 2002). The importance of the linker domain in modulating the enzyme dynamics has been established from a series of experiments carried out on an enzyme having an altered linker domain. In fact, comparison of the catalytic properties of the topo70 enzyme and those of a), the linker deleted form topo58/6.3 (Stewart et al., 1997); b), the topo58/12 form, in which the linker domain is not covalent bonded to the core domain (Stewart et al., 1999); c), the topo70ΔL enzyme, having the region 660–688 deleted, resulting in a shortened linker domain (Ireton et al., 2000); and d), the single Ala-653Pro mutation on the linker domain (Fiorani et al., 2003) indicates that all ''linker-disabled'' topoisomerase forms exhibit:

1. Slight reduction in activity.
2. A cleavage-religation equilibrium shifted toward the relegation.
3. Reduced DNA binding affinity.
4. Distributive relaxation mode, where the modified enzymes appear to leave the DNA substrate after removing only a few supercoils at a time.
5. Camptothecin resistance.

Taken together, these observations indicate that the linker domain perturbs the enzyme dynamics by slowing the religation step of catalysis, permitting the wild-type enzyme to remain covalently bound to DNA and enhancing CPT's ability to stabilize the covalent protein-DNA intermediate (Fiorani et al., 2003).

Specific motions detected in our simulations can be directly correlated with experimental results reported in the literature. In detail, in our simulation residues 203–214 of the N-terminal domain, included in the model, show a disjoined dynamics from the core domain. The order parameter S^2 (Fig. 3) indicates significant flexibility of the Glu-213/Gly-214

backbone, whereas the dynamic correlation map (Fig. 4) shows correlated movement between residues 203–208 and four key protein regions: helix 8 in core subdomain III (highlighted in *ellipse A*); the N-terminal portion of helix 19 in the linker domain (highlighted in *ellipse B*); the catalytic region around Tyr-723; and helices 22 and 23 in the C-terminal domain (highlighted in *ellipse C*). The flexibility of the Glu-213/Gly-214 backbone, therefore, seems critical to the involvement of the N-terminal residues 203–208 to protein communications among essential topoisomerase regions. Indeed, the influence of the N-terminal residues 191–206 on the enzyme's catalytic cycle has been elucidated by biochemical experiments (Lisby et al., 2001; Christensen et al., 2003). Recently, the 203–206 region, and in particular Trp-205, has been shown to participate in the control of the DNA rotation step (Frohlich et al., 2004), likely by coordinating the function of the linker domain or the nose cone helices, as was suggested on the basis of structural data (Redinbo et al., 2000). Our simulation indicates that this coordinated function can be exerted through the correlation of the linker domain and the 203–206 N-terminal residues.

The lip1 (Phe-361–Lys-369), one of the two lips that closes the clamp around the DNA, exhibits significantly different dynamics in topo70 when compared to topo58/6.3. Arg-364, in particular, shows larger fluctuations (Fig. 2) and a more flexible backbone (Fig. 3) in topo70. Indeed, the 364–365 region of topoisomerase I has been shown to influence both the enzymatic activity of the enzyme (Li et al., 1997; Fiorani et al., 1999) and the efficacy of the camptothecins (Benedetti et al., 1993; Rubin et al., 1994; Li et al., 1997; Bailly et al., 1999; Fiorani et al., 1999; Urasaki et al., 2001; Chrencik et al., 2004).

Finally, our simulations strongly reinforce the hypothesis that helix 8 may play a role in the opening and closing of the enzyme around DNA (Redinbo et al., 2000). In fact this helix shows correlated or anticorrelated motions with the following key protein regions: the 203–208 N-terminal residues; the central portion of the linker domain; nearly the whole C-terminal domain; and helix 16 in core subdomain III, which contains the catalytic Arg-590. The wider fluctuations and the absence of such correlated motions in the topo58/6.3 system may account for the distributive behavior of 58/6.3 relative to the processive nature of topo70, i.e., only the whole form of the enzyme can accurately control the opening-closing of the enzyme around DNA.

Several aspects of human topoisomerase I dynamics in relation to function still remain to be examined, however. One example is the flexibility of the enzyme's active site and C-terminal domain in the absence of DNA. It has recently been shown that the presence of an 8-oxoguanine site of DNA damage in a DNA duplex causes the catalytic tyrosine residue of human topoisomerase I to rotate away from the remaining active site residues (Lesher et al., 2002). Such a rearrangement is reminiscent of the tyrosine recombinases and integrases that have also been shown to dock their catalytic tyrosines away from their active site residues, perhaps to regulate enzyme catalysis (Guo et al., 1997; Kwon et al., 1997; Subramanya et al., 1997; Chen et al., 2000). The C-terminal domain of topo70 remains relatively rigid in the simulations presented here in the presence of DNA. It would be of interest to examine whether the active site or C-terminal domain of human topoisomerase I is more dynamic in the absence of DNA.

The authors thank Jill Chrencik for preparing Fig. 1, *A* and *B*. We acknowledge the CASPUR Computational Center for the computer architecture used in this work.

This work was partly supported by grants from MURST COFIN2003, from Ministero della Salute, and by a FIRB project on Bioinformatics for Genomics and Proteomics.

REFERENCES

Andoh, T., K. Ishii, Y. Suzuki, Y. Ikegami, Y. Kusunoki, Y. Takemoto, and K. Okada. 1987. Characterization of a mammalian mutant with a camptothecin resistant DNA topoisomerase I. *Proc. Natl. Acad. Sci. USA.* 84:5565–5569.

Bailly, C. 2003. Homocamptothecins: potent topoisomerase I inhibitors and promising anticancer drugs. *Crit. Rev. Oncol. Hematol.* 45:91–108.

Bailly, C., C. Carrasco, F. Hamy, H. Vezin, M. Prudhomme, A. Saleem, and E. Rubin. 1999. The camptothecin-resistant topoisomerase I mutant F361s is cross-resistant to antitumor rebeccamycin derivatives. A model for topoisomerase I inhibition by indolocarbazoles. *Biochem.* 38:8605–8611.

Benedetti, P., P. Fiorani, L. Capuani, and J. C. Wang. 1993. Camptothecin resistance from a single mutation changing glycine 363 of human DNA topoisomerase I to cysteine. *Cancer Res.* 53:4343–4348.

Berendsen, H. J. C., J. P. M. Postma, W. F. van Gusteren, A. Di Nola, and J. R. Haak. 1984. Molecular dynamics with coupling to an external bath. *J. Comput. Phys.* 81:3684–3690.

Berendsen, H. J. C., D. van der Spool, and R. van Drunen. 1995. GROMACS: a message-passing parallel molecular dynamics implementation. *Comp. Phys. Comm.* 95:43–56.

Carey, J. F., S. J. Schultz, L. Sission, T. G. Fazzio, and J. J. Champoux. 2003. DNA relaxation by human topoisomerase I occurs in the closed clamp conformation of the protein. *Proc. Natl. Acad. Sci. USA.* 100:5640–5645.

Cheatham, T. E., J. L. Miller, T. Fox, T. A. Darden, and P. A. Kollman. 1995. Molecular dynamics simulation on solvated biomolecular systems: the particle mesh Ewald method leads to stable trajectories of DNA, RNA and proteins. *J. Am. Chem. Soc.* 117:4193–4194.

Chen, Y., U. Narendra, L. E. Iype, M. M. Cox, and P. A. Rice. 2000. Crystal structure of a Flp recombinase-Holliday junction complex: assembly of an active oligomer by helix swapping. *Mol. Cell.* 6:885–897.

Chillemi, G., T. Castrignanò, and A. Desideri. 2001. Structure and hydration of the DNA-human topoisomerase I covalent complex. *Biophys. J.* 81:490–500.

Chillemi, G., P. Fiorani, P. Benedetti, and A. Desideri. 2003. Protein concerted motions in the DNA-human topoisomerase I complex. *Nucleic Acids Res.* 31:1525–1535.

Chrencik, J. E., A. B. Burgin, Y. Pommier, L. Stewart, and M. R. Redinbo. 2003. Structural impact of the leukemia drug Ara-C on the covalent human topoisomerase I DNA complex. *J. Biol. Chem.* 278:12461–12466.

Chrencik, J. E., B. L. Staker, A. B. Burgin, P. Pourquier, Y. Pommier, L. Stewart, and M. R. Redinbo. 2004. Mechanisms of camptothecin resistance by human topoisomerase I mutations. *J. Mol. Biol.* 339:773–784.

Christensen, M. O., H. U. Barthelmes, F. Boege, and C. Mielke. 2003. Residues 190–210 of human topoisomerase I are required for enzyme activity in vivo but not in vitro. *Nucleic Acids Res.* 31:7255–7263.

Cornell, W. D., P. Cieplak, C. I. Bayly, I. R. Gould, M. Kenneth, J. Merz, D. M. Ferguson, D. C. Spellmeyer, T. Fox, J. W. Caldwell, and P. A. Kolman. 1995. A second generation force field for the simulation of proteins, nucleic acids, and organic molecules. *J. Am. Chem. Soc.* 117:5179–5197.

Darden, T., D. York, and L. Pedersen. 1993. Particle mesh Ewald: an N.log(n) method for Ewald sums in large systems. *J. Chem. Phys.* 98:10089–10092.

Fertala, J., J. R. Vance, P. Pourquier, Y. Pommier, and M.-A. Bjornsti. 2000. Substitutions of Asn-726 in the Active Site of Yeast DNA Topoisomerase I Define Novel Mechanisms of Stabilizing the Covalent Enzyme-DNA Intermediate. *J. Biol. Chem.* 275:15246–15253.

Fiorani, P., J. F. Amatruda, A. Silvestri, R. H. Butler, M.-A. Bjornsti, and P. Benedetti. 1999. Domain Interactions Affecting Human DNA Topoisomerase I Catalysis and Camptothecin Sensitivity. *Mol. Pharmacol.* 56:1105–1115.

Fiorani, P., A. Bruselles, M. Falconi, G. Chillemi, A. Desideri, and P. Benedetti. 2003. Single mutation in the linker domain confers protein flexibility and camptothecin resistance to human topoisomerase I. *J. Biol. Chem.* 278:43268–43275.

Frohlich, R. F., F. F. Andersen, O. Westergaard, A. H. Andersen, and B. R. Knudsen. 2004. Regions within the N-terminal domain of human topoisomerase I exert important functions during strand rotation and DNA binding. *J. Mol. Biol.* 336:93–103.

Giudice, E., and R. Lavery. 2002. Simulations of nucleic acids and their complexes. *Acc. Chem. Res.* 35:350–357.

Guo, F., D. N. Gopaul, and G. D. van Duyne. 1997. Structure of Cre recombinase complexed with DNA in a site-specific recombination synapse. *Nature.* 389:40–46.

Hann, C., D. L. Evans, J. Fertala, P. Benedetti, M.-A. Bjornsti, and D. J. Hall. 1998. Increased camptothecin toxicity induced in mammalian cells expressing saccharomyces cerevisiae DNA topoisomerase I. *J. Biol. Chem.* 273:8425–8433.

Interthal, H., P. M. Quigley, W. G. J. Hol, and J. J. Champoux. 2004. The role of lysine 532 in the catalytic mechanism of human topoisomerase I. *J. Biol. Chem.* 279:2984–2992.

Ireton, G. C., L. Stewart, L. H. Parker, and J. J. Champoux. 2000. Expression of human topoisomerase I with a partial deletion of the linker region yields monomeric and dimeric enzymes that respond differently to camptothecin. *J. Biol. Chem.* 275:25820–25830.

Jorgensen, W. L., J. Chandrasekhar, J. D. Madura, R. W. Impey, and M. L. Klein. 1983. Comparison of simple potential functions for simulating liquid water. *J. Chem. Phys.* 79:926–935.

Knab, A. M., J. Fertala, and M.-A. Bjornsti. 1993. Mechanisms of camptothecin resistance in yeast DNA topoisomerase I mutants. *J. Biol. Chem.* 268:22322–22330.

Knab, A. M., J. Fertala, and M.-A. Bjornsti. 1995. A Camptothecin-resistant DNA topoisomerase I mutant exhibits alteres sensitivities to other DNA topoisomerase poisons. *J. Biol. Chem.* 270:6141–6148.

Kwon, H. J., R. Tirumalai, A. Landy, and T. Ellenberger. 1997. Flexibility in DNA recombination: structure of the lambda integrase catalytic core. *Science.* 276:126–131.

Laco, G. S., J. R. Collins, B. T. Luke, H. Kroth, J. M. Sayer, D. M. Jerina, and Y. Pommier. 2002. Human topoisomerase I inhibition: docking camptothecin and derivatives into a structure-based active site model. *Biochem.* 41:1428–1435.

Lesher, D. T., Y. Pommier, L. Stewart, and M. R. Redinbo. 2002. 8-oxoguanine rearranges the active site of human topoisomerase I. *Proc. Natl. Acad. Sci. USA.* 99:12102–12107.

Leteurtre, F., A. Fujimori, A. Tanizawa, A. Chhabra, A. Mazumder, G. Kohlhagen, H. Nakano, and Y. Pommier. 1994. Saintopin, a dual inhibitor of DNA topoisomerase I and II, as a probe for drug-enzyme interactions. *J. Biol. Chem.* 269:28702–28707.

Li, X. G., P. Haluska, Y.-H. Hsiang, A. K. Bharti, D. W. Kufe, L. F. Liu, and E. H. Rubin. 1997. Involvement of amino acids 361 to 364 of human topoisomerase I in camptothecin resistance and enzyme catalysis. *Biochem. Pharmacol.* 53:1019–1027.

Lisby, M., J. R. Olesen, C. Skouboe, B. O. Krogh, T. Straub, F. Boege, S. Velmurugan, P. M. Martensen, A. H. Andersen, M. Jayaram, O. Westergaard, and B. R. Knudsen. 2001. Residues within the N-terminal domain of human topoisomerase I play a direct role in relaxation. *J. Biol. Chem.* 276:20220–20227.

MacKerell, A. D., and L. Nilsson. 2001. Nucleic acid simulations. *In* Computational Biochemistry and Biophysics. O. Becker, A. D. MacKerell, B. Roux, and M. Watanabe, editors. Marcel Dekker, New York.

Mc Cammon, J. A., and S. C. Harvey. 1987. Dynamics of Proteins and Nucleic Acids. Cambridge University Press, London.

Pommier, Y., P. Pourquier, Y. Fan, and D. Strumberg. 1998. Mechanism of action of eukaryotic DNA topoisomerase I and drugs targeted to the enzyme. *Biochim. Biophys. Acta.* 1400:83–106.

Pommier, Y., P. Pourquier, Y. Urasaki, J. Wu, and G. S. Laco. 1999. Topoisomerase I inhibitors: selectivity and cellular resistance. *Drug Resist. Updat.* 2:307–318.

Pommier, Y., C. Redon, V. A. Rao, J. A. Seiler, O. Sordet, H. Takemura, S. Antony, L. H. Meng, Z. Y. Liao, G. Kohlhagen, H. L. Zhang, and K. W. Kohn. 2003. Repair of and checkpoint response to topoisomerase I-mediated DNA damage. *Mutat. Res.* 532:173–203.

Reddy, S. Y., S. Obika, and T. C. Bruice. 2003. Conformations and dynamics of Ets-1 ETS domain-DNA complexes. *Proc. Natl. Acad. Sci. USA.* 100:15475–15480.

Redinbo, M. R., J. J. Champoux, and W. G. J. Hol. 2000. Novel Insight into catalytic mechanism from a crystal structure of human topoisomerase I in complex with DNA. *Biochemistry.* 39:6832–6840.

Redinbo, M. R., L. Stewart, J. J. Champoux, and W. G. J. Hol. 1999. Structural flexibility in human topoisomerase I revealed in multiple nonisomorphous crystal structures. *J. Mol. Biol.* 292:685–696.

Redinbo, M. R., L. Stewart, P. Kuhn, J. J. Champoux, and W. G. J. Hol. 1998. Crystal structures of human topoisomerase I in covalent and noncovalent complexes with DNA. *Science.* 279:1504–1513.

Rubin, E., P. Pantazis, A. Bharti, D. Toppmeyer, B. Giovannella, and D. Kufe. 1994. Identification of a mutant topoisomerase I with intact catalytic activity and resistance to 9-nitro-camptothecin. *J. Biol. Chem.* 269:2433–2439.

Ryckaert, J.-P., G. Ciccotti, and H. J. C. Berendsen. 1977. Numerical integration of the Cartesian equations of motion of a system with constraints: molecular dynamics of n-alkanes. *J. Comput. Phys.* 23:327–341.

Saleem, A., N. Ibrahim, M. Patel, X. G. Li, E. Gupta, J. Mendoza, P. Pantazis, and E. H. Rubin. 1997. Mechanisms of resistance in a human cell line exposed to sequential topoisomerase poisoning. *Cancer Res.* 57:5100–5106.

Staker, B. L., K. Hjerrild, M. D. Feese, C. A. Behnke, A. B. Burgin, and L. Stewart. 2002. The mechanism of topoisomerase I poisoning by a camptothecin analog. *Proc. Natl. Acad. Sci. USA.* 99:15387–15392.

Stewart, L., G. Ireton, and J. Champoux. 1997. Reconstitution of human topoisomerase I by fragment complementation. *J. Mol. Biol.* 269:355–372.

Stewart, L., G. Ireton, and J. Champoux. 1999. A Functional linker in human topoisomerase I is required for maximum sensitivity to camptothecin in a DNA relaxation assay. *J. Biol. Chem.* 274:32950–32960.

Stewart, L., M. R. Redinbo, X. Qiu, W. G. J. Hol, and J. J. Champoux. 1998. A model for the mechanism of human topoisomerase I. *Science.* 279:1534–1541.

Subramanya, H. S., L. K. Arciszewska, R. A. Baker, L. E. Bird, D. J. Sherratt, and D. B. Wigley. 1997. Crystal structure of the site-specific recombinase, XerD. *EMBO J.* 16:5178–5187.

Tamura, H., C. Kohchi, R. Yamada, T. Ikeda, O. Koiwai, E. Patterson, J. D. Keene, K. Okada, E. Kjeldsen, K. Nishikawa. 1991. Molecular cloning of a cDNA of a camptothecin-resistant human DNA topoisomerase I and identification of mutation sites. *Nucleic Acids Res.* 19:69–75.

Tsui, V., I. Radhakrishnan, P. E. Wright, and D. A. Case. 2000. NMR and molecular dynamics studies of the hydration of a zinc finger-DNA complex. *J. Mol. Biol.* 302:1101–1117.

Urasaki, Y., G. S. Laco, P. Pourquier, Y. Takebayashi, G. Kohlhagen, C. Gioffre, H. Zhang, D. Chatterjee, P. Pantazis, and Y. Pommier. 2001. Characterization of a novel topoisomerase I mutation from a camptothecin-resistant human prostate cancer cell line. *Cancer Res.* 61:1964–1969.

Van der Spoel, D., and H. J. C. Berendsen. 1997. Molecular dynamics simulations of leu-enkephalin in water and DMSO. *Biophys. J.* 72:2032–2041.

Woo, M. H., C. Losasso, H. Guo, L. Pattarello, P. Benedetti, and M. A. Bjornsti. 2003. Locking the DNA topoisomerase I protein clamp inhibits DNA rotation and induces cell lethality. *Proc. Natl. Acad. Sci. USA.* 100:13767–13772.